Computer Communications 145 (2019) 146–160

Contents lists available at ScienceDirect

Computer Communications

journal homepage: www.elsevier.com/locate/comcom

Multi-population coevolutionary dynamic multi-objective particle swarm optimization algorithm for power control based on improved crowding distance archive management in CRNs

Lingling Chen [a,b,c,*], Qi Li [a], Xiaohui Zhao [c], Zhiyi Fang [b], Furong Peng [a], Jiaqi Wang [a]

[a] College of Information and Control Engineering, Jilin Institute of Chemical Technology, Jilin, Jilin, 130022, China
[b] School of Computer Science, Jilin University, Changchun, Jilin, 130012, China
[c] Key Laboratory of Information Science, College of Communication Engineering, Jilin University, Changchun, Jilin, 130012, China

ARTICLE INFO

Keywords:
Cognitive radio networks
Underlay
Power control algorithm
Dynamic communication environment
The improved coevolutionary multi-objective particle swarm algorithm

ABSTRACT

This paper aims to resolve the problem of power control in underlay CRNs better. Firstly, a multi-objective optimization problem of maximizing the throughput of PUs and SUs is proposed, which satisfied the constraints of PU' interference temperature, the normal communication quality of all users and the transmission power limitation of users. Moreover, according to the theory of penalty function and particle swarm optimization (PSO), an improved multi-objective particle swarm optimization (IMOPSO) algorithm is proposed based on the archives management, which can achieve the maximum throughput of PUs and SUs as well as the minimum penalty constraints term. On this basis, in order to improve the boundary searching ability and diversity of the power control scheme, an improved coevolutionary multi-objective particle swarm optimization (ICMOPSO) in multiple population is proposed based on crowding distance archival management. Further, in order to adapt to the dynamic communication environment well, three different dynamic response schemes are presented correspondingly to cope with the instability of three types of environment. In the end, simulation results show that ICMOPSO and IMOPSO algorithm based on the archives management can obtain the maximum throughput compared with the conventional PSO. Through comparing with the performances in IMOPSO and ICMOPSO, it can be concluded that ICMOPSO algorithm has good abilities of stability, diversity and local search ability, which can provide more throughput optimal allocation schemes for decision makers and ensure the quality of customer service. On the basis of ICMOPSO algorithm, dynamic response strategy is better than the static response strategy at computational cost compared with the average number of iterations. And it can cope with the dimensional change of decision space in dynamic communication environment.

1. Introduction

With the rapid development of wireless communication, the existing spectrum resources have been unable to meet the growing demand. In order to enhance the spectrum efficiency and solve the shortage of the spectrum, cognitive radio technology was proposed [1]. This technology can be used in intelligent detection of spectrum resources, searching for available spectrum resources (spectrum hole), and adjustment of transmission power of primary users (PUs) and secondary users (SUs), so as to realize spectrum sharing. Therefore, power control is one of the core technologies in cognitive radio network system.

Currently, swarm intelligence algorithms [2–5] have been commonly applied to power control. In underlay cognitive radio networks (CRNs), considered of PUs' interference constraint and ensured the communication quality of SUs, an improved artificial fish swarm algorithm was proposed to realize the optimization goal of minimizing the secondary user transmitter (SU-Tx) to primary user receiver (PU-Rx) total interference in [2]. However, the method only reduces the total interference of SU-Tx to PU-Rx, which cannot consider the optimal communication quality of each PU. The reference [3] proposed to minimize the sum of all the SU-Txs transmission powers, and utilize chaotic particle swarm algorithm to solve the optimization problems under the constraints of satisfying the minimum SINR, maximum transmission power and the maximum permissible interference of PU. Energy consumption of SUs can be reduced in this method, which can merely ensure normal communication. In reference [4], in order to meet the minimizing all of SU-Tx transmission powers, a dynamic particle swarm optimization was proposed to adapt the dynamic communication environment under the constraints on guaranteeing PU-Rx interference temperature, SINR of SU-Rx and transmission power. In cognitive networks, to deal with the power allocation problem of multiple input and

* Correspondence to: 45 Chengde Street, Jilin City, Jilin Province, 132022, China.
E-mail address: linglingchen@jlict.edu.cn (L. Chen).

https://doi.org/10.1016/j.comcom.2019.06.009
Received 15 March 2018; Received in revised form 12 February 2019; Accepted 19 June 2019
Available online 27 June 2019

multiple output orthogonal frequency division multiplex systems, the sum of SUs' power is minimized by population-adaptive differential evolution algorithm in reference [5]. All above swarm intelligence algorithms are used to solving the single objective problem of power control in cognitive radio network. However, in actual communication situation, the needs of PUs and SUs should be taken into consideration from different angles.

As far as we know, there are lots of multi-objectives swarm intelligent algorithms [6] which have applied to the spectral sensing [7,8] in CRNs. In order to maximize throughput and minimize total interference from secondary users to primary users, a linear weighted multi-objective particle swarm optimization algorithm is proposed to deal with wideband spectrum sensing problem of OFDM CRNs by [7]. The paper [8] considers the multi-objective optimization problem that minimizes the forced termination probability along with three utility functions namely Max-Sum-Reward, Max-Min-Reward and Max-Proportional-Fair to improve the quality of service. In order to achieve the goal, a spectrum allocation algorithm based on multi-objective differential evolution is proposed under the constraints of selecting the number and capacity of the required channel in the cognitive radio network. In summary, the advantages of the multi-objective swarm intelligent algorithms are more consistent with the needs of the actual users.

However, there are only a few on multi-objective swarm intelligent algorithms which have been applied to power control in CRNs. In reference [9], the CR parameter adaptation problem is established and transformed into an unconstrained multi-objective optimization problem in a multicarrier system. Moreover, a non-dominated front searching algorithm based on user preference (NFSA-UP) is proposed to determine the optimal transmission parameters. NFSA-UP is compared with other pareto front searching algorithms NSGAII and NSGAII-LBS (Light Beam Search based on NSGAII), and the results demonstrate that the optimal transmission parameters of CR can be got using NFSA-UP with any user preference direction, while better performance is observed. But this method only considers unconstrained multi-carrier optimal power control problem.

In addition, the study of multi-objective optimization problem is also essential in the time-varying environment. Because the parameters are variable with the changeable environment in system, which causes the changes of the optimal solution and traps into local optimum. In reference [10], the dynamic environment is detected by sentinel particle. However, the selected sentinel particles are easily to flock together for PSO algorithm in part space, which leads to the failure of realizing global monitor and occurrence of misjudgment. Therefore, only detecting the change of system environment is not enough to improve the convergence speed in multi-objective algorithm. In reference [11], after the changes in the environment, Deb proposed two optimization schemes to increase the diversities of solutions by NSGAII. But the standards of environmental change intensity are difficult to be determined. In reference [12], four kinds of response strategies were given to cope with the changeable environment. But it was difficult to give the prediction information on environment. When the environment is changing, the Kalman filter model is instructed to predict the descendant Pareto optimal solution according to the historical Pareto frontier, and a scoring scheme is designed by combining the Kalman filter prediction model with the random initialization strategy to improve the prediction performance based on the multi-objective differential evolution algorithm in the paper [13]. But there is no detailed answer to the constraint problem. In this paper [14], on the basis of differential evolution (DE) algorithm, a new dynamic evolutionary approach is proposed to adapt the new environmental condition, which is using variable relocation. The newly adapted population is shown to be fitter to the new environment than the original or most randomly generated population. In the paper [15], a multi-objective differential evolution decomposition algorithm (IM-MOEA) is proposed to simplify the targeted subspace assignment of different inverse models by using the weight vector of MOEA/D. The inverse model is utilized to detect the changes of objective function to search for potential decision subspace regions. Different from the inversion model, the decision variables are divided into two sub-components according to the relationship between the decision variables and the environment in the paper [16]. Then the two sub-components are collaboratively optimized on the basis of MOEA. Then the two prediction methods, differential prediction and Cauchy mutation, are used to speed up their response in the changed environment. The performance of the above multi-objective optimization algorithm is superior, which have been considered the dynamic environments. But the working state of user is unpredictable in cognitive radio network, and the space dimension change of multi-objective decision-making can be insufficient attention.

Based on the above considerations, regarding the underlay cognitive radio networks in which PUs and SUs share the same frequency band, a multi-objective optimization problem of maximizing the throughput [17] of PUs and SUs is proposed in this paper under the premise of satisfying each PU' interference temperature [18], guaranteeing normal communication of all users and meeting transmission power limitation of user. Moreover, according to the theory of penalty function and PSO, two types of power control algorithms (IMOPSO and ICMOPSO) based on the archives management were proposed to achieve the maximum throughput of PUs and SUs as well as the minimum penalty constraints term. Then, in order to well adapt to the actual communication environment, the types and status of the changeable environment was monitored by the improved sentinel particles. On this foundation, the corresponding dynamic responses strategies are proposed based on the ICMOPSO algorithm. Finally, simulation results show that ICMOPSO and IMOPSO algorithm based on the archives management can ensure normal communication for all users and obtain the maximum throughput of PUs and SUs. Through comparing with the performances of crowding variance (CV) [19], generation distance (GD) [19] and maximum spread (MS) [20] in IMOPSO, ICMOPSO, it can be concluded that ICMOPSO algorithm had the good stability, diversity and local search ability, which can provide more throughput optimal allocation schemes for decision makers and ensure the quality of service (QoS) of user. On the basis of ICMOPSO algorithm, dynamic response strategy is better than the static response strategy at computational cost by comparing with the average number of iterations in each type of the changeable environment, which is under the same constraints of CV, GD and MS. And it can cope with the dimensional change of decision space in dynamic communication environment.

This paper is organized as follows. In Section 2, the system model is described in underlay cognitive radio network. In order to obtain the maximum throughput of PUs and SUs, the power control scheme is proposed by IMOPSO and ICMOPSO algorithms. Moreover, for adapting to the three types of the dynamic environments, three dynamic response strategies based on ICMOPSO are proposed in Section 3. The simulation results are shown in Section 4. Finally, Section 5 summarizes the conclusions of this paper.

2. System model

High-capacity wireless communication networks are characterized by the reuse of the available frequency band. Therefore, we consider an underlay scenario of this paper, where has transmitter–receiver pairs of N PUs and transmitter–receiver pairs of M SUs in cognitive radio network as shown Fig. 1.

In order to ensure the communication reliability of the PUs, the total interference of all SU-Txs to PU-Rx should not exceed the follow interference temperature.

$$\sum_{s=N+1}^{N+M} P_s K_{si} \le I_i \tag{1}$$

Where P_s is the transmission power of SU-Tx on link $s\,(s \in F)$, and $F = \{N+1, N+2, \ldots, N+M\}$ denotes a set of sub channels, which

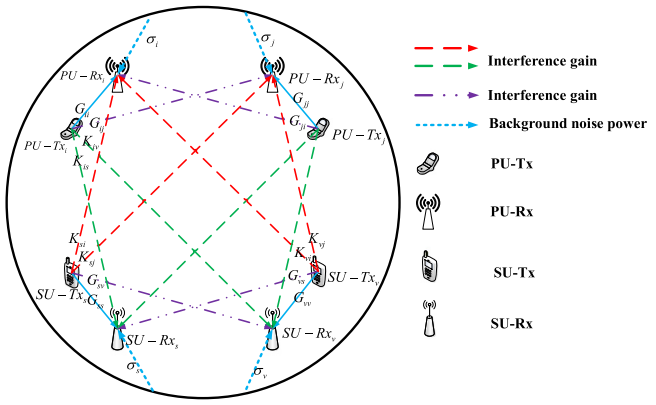

Fig. 1. Multiuser distributed CNRs.

is used by all SUs. $N + M$ represents the total number of the PUs and SUs. K_{si} denotes the interference gain from the SU-Tx on link s to the PU-Rx on link $i\,(i \in D)$, and $D = \{1, 2, \ldots, N\}$ is ordinal number of the PUs. I^i is the maximum tolerable interference power of the PU-Rx on link i, namely the interference temperature.

In order to guarantee the QoS requirements of both PUs and SUs, the actual SINR of the PU-Rxs and SU-Rxs must exceed the corresponding threshold

$$\gamma_i \geq \gamma_i^* \tag{2}$$

$$\gamma_s \geq \gamma_s^* \tag{3}$$

Where γ_i^* denotes the SINR threshold of the PU-Rx on link i. γ_s^* represents the SINR threshold of the SU-Rx on link s. Considering the influence of the PUs and SUs interference and background noise, the actual SINR of the PU-Rx on link i and the actual SINR of the SU-Rx on link s can be defined as

$$\gamma_i = \frac{P_i G_{ii}}{\sigma_i + \sum_{i \neq j} P_j G_{ji} + \sum_{s=N+1}^{N+M} P_s K_{si}} \tag{4}$$

$$\gamma_s = \frac{P_s G_{ss}}{\sigma_s + \sum_{s \neq v} P_v G_{vs} + \sum_{i=1}^{N} P_i K_{is}} \tag{5}$$

Where P_i is the transmission power of the PU-Tx on link i. P_j denotes the transmission power of the PU-Rx on link $j\,(j \in D)$. G_{ii} represents the direct channel gain of the PU-Tx to PU-Rx on link i. G_{ji} is interference gain from PU-Tx on link j to the PU-Rx on link i. $\sum_{i \neq j} P_j G_{ji}$ denotes the total interference from other PU-Tx to PU-Rx on link i. P_v represents the transmission power of SU-Tx at link $v\,(v \in F)$. G_{ss} is the direct channel gain from SU-Tx to SU-Rx on link s. G_{vs} denotes the interference gain from SU-Tx on link v to SU-Rx on link s. $\sum_{s \neq v} P_v G_{vs}$ represents the total interference from other SU-Tx to SU-Rx on link s. $\sum_{s=N+1}^{N+M} P_s K_{si}$ is the total interference from SU-Txs to PU-Rx on link i. K_{is} denotes the interference gain from PU-Tx on link i to SU-Rx on link s. $\sum_{i=1}^{N} P_i K_{is}$ represents the total interference from PU-Txs to SU-Rx on link s. σ_i represents the background noise power of the PU-Rx on link i. σ_s is the background noise power of the SU-Rx on link s.

Consider the limitation of battery equipment, the transmission power of each user is given as

$$0 \leq P_i \leq P_i^{\max} \tag{6}$$

$$0 \leq P_s \leq P_s^{\max} \tag{7}$$

Where $P_i^{\max}$ denotes the maximum transmission power of the PU-Tx on link i. $P_s^{\max}$ represents the maximum transmission power of the SU-Tx on link s.

In order to achieve optimal resource allocation and ensure normal communication, an optimized model that maximizes the throughput of the PUs and SUs was established under the above constraints

$$\begin{cases} \max \sum_{i=1}^{N} \log\left(1+\gamma_i\right) \\ \max \sum_{s=N+1}^{N+M} \log\left(1+\gamma_s\right) \\ \begin{cases} C1: \sum_{s=N+1}^{N+M} P_s K_{si} \leq I_i \\ C2: \gamma_i \geq \gamma_i^* \\ C3: \gamma_a \geq \gamma_a^* \\ C4: 0 \leq P_i \leq P_i^{\max} \\ C5: 0 \leq P_s \leq P_s^{\max} \end{cases} \end{cases} \tag{8}$$

Where $\sum_{i=1}^{N} \log\left(1+\gamma_i\right)$ and $\sum_{s=N+1}^{N+M} \log\left(1+\gamma_s\right)$ is throughput of PUs and SUs, respectively. $C1$ denotes total interference power that is less than the interference temperature level to guarantee the QoS of PUs. $C2$ represents the minimum SINR constraint for each PU-Rx to ensure the QoS of each PU. $C3$ is the minimum SINR constraint for each SU-Rx to guarantee the QoS of each SU. $C4$ denotes the transmit power range of PU-Txs. $C5$ represents the transmit power range of SU-Txs.

3. Power control

In this chapter, the above problem (8) of the PUs and SUs power control is solved by IMOPSO and ICMOPSO, respectively. In addition, considered the change of the communication environment, three different dynamic response strategies based on ICMOPSO algorithm were proposed to cope with the instability of dynamic communication system.

3.1. Power control algorithm based on IMOPSO

According to the penalty theory [21], the constraints $C1$, $C2$ and $C3$ of model (8) were transformed into a new objective, which is defined as the index of violating normal communication (VNC). The smaller VNC is, the better the user's communication stability is. The power optimization model (8) is processed as follows

$$\begin{cases} \max \sum_{i=1}^{N} \log\left(1+\gamma_i\right) \\ \max \sum_{s=N+1}^{N+M} \log\left(1+\gamma_s\right) \\ \min \sum_{i=1}^{N} \left\langle \gamma_i - \gamma_i^* \right\rangle + \sum_{i=1}^{N} \left\langle I_i - \sum_{s=N+1}^{N+M} P_s K_{si} \right\rangle + \sum_{s=N+1}^{N+M} \left\langle \gamma_s - \gamma_s^* \right\rangle \\ \text{s.t.} \begin{cases} 0 \leq P_i \leq P_i^{\max} \\ 0 \leq P_s \leq P_s^{\max} \end{cases} \end{cases} \tag{9}$$

If $\gamma_s - \gamma_s^* \geq 0$ holds, $\left\langle \gamma_i - \gamma_i^* \right\rangle$ is set zero. Otherwise, $\left\langle \gamma_s - \gamma_s^* \right\rangle = -\left(\gamma_s - \gamma_s^*\right) > 0$. Similarly, the $I^i - \sum_{s=N+1}^{N+M} P_s K_{si}$ and the $\gamma_i - \gamma_i^*$ is suitable for the above situation.

When VNC is equal to 0, all users are able to work properly. According to the model (9) and the IMOPSO algorithm, the above problem (8) can be converted to the fitness function as follows

$$F(P) = \begin{cases} f_{PU}(P) = \sum_{i=1}^{N} \log\left(1+\gamma_i\right) \\ f_{SU}(P) = \sum_{a=N+1}^{N+M} \log\left(1+\gamma_s\right) \\ f_{VNC}(P) = \sum_{i=1}^{N} \left\langle \gamma_i - \gamma_i^* \right\rangle + \sum_{i=1}^{N} \left\langle I_i - \sum_{s=N+1}^{N+M} P_s K_{si} \right\rangle + \sum_{s=N+1}^{N+M} \left\langle \gamma_s - \gamma_s^* \right\rangle \end{cases} \tag{10}$$

Where $F(P)$ denotes the value of fitness function and the food concentration. $P = \left(P_1, \ldots, P_i, \ldots, P_N, P_{N+1}, \ldots, P_s, \ldots, P_{N+M}\right)$ is a set of the

transmission power of user transmitter, which also represents position of particles in the IMOPSO algorithm. $f_{PU}(P)$ represents the throughput of all PUs and the concentration of beneficial food A. $f_{SU}(P)$ denotes the throughput of all SUs and the concentration of beneficial food B. $f_{VNC}(P)$ is the VNC and the concentration of the harmful food C. When the concentration of the food A and B are maximized, and the concentration of the food C is minimized simultaneously, a set of optimal power control schemes can be obtained. Moreover, it is worth noting that if the concentration of the food C is greater than 0, the particles are active in the toxic food region and the situations do not meet constrains. To prevent the particles from being poisoned, the concentration of the food C is regarded as a merits prerequisite in the determination of the multi-objective dominance relationship, namely the particle of $f_{VNC}(P) = 0$ dominate the particle of $f_{VNC}(P) \neq 0$ in any cases.

In addition, according to the theory of PSO [22], we can clearly know that the fitness function, the position and the velocity can be depicted as characteristics of every particle. Thus, the position and the velocity of particle l in the tth iteration can be expressed as

$$\begin{aligned} xP^{l,t} &= \left(xP_1^{l,t}, \ldots, xP_h^{l,t}, \ldots, xP_{N+M}^{l,t}\right) \\ &= \left(xP_1^{l,t}, \ldots, xP_i^{l,t}, \ldots, xP_N^{l,t}, xP_{N+1}^{l,t}, \ldots, xP_s^{l,t}, \ldots, xP_{N+M}^{l,t}\right) \end{aligned} \tag{11}$$

Where $xP_h^{l,t}$ represents the hth ($h \in DF$) dimension position of the particle l in the tth iteration, and denotes the transmission power of the user on link h.$DF = \{1, 2, \ldots, N+M\}$ denotes the set of dimensions in the particle location and the set of sub channels for all users. $xP_i^{l,t}$ is the ith dimension position of the particle l in the tth iteration and the transmission power of PU's transmitter on link i.$xP_s^{l,t}$ represents the sth dimension position of the particle l in the tth iteration and the transmission power of the SU's transmitter on link s. Therefore, the fitness function of the particle l in the tth iteration is expressed as

$$F\left(xP^{l,t}\right) = \begin{cases} f_{PU}\left(xP^{l,t}\right) = \sum_{i=1}^{N} \log\left(1+\gamma_i^{l,t}\right) \\ f_{SU}\left(xP^{l,t}\right) = \sum_{s=N+1}^{N+M} \log\left(1+\gamma_s^{l,t}\right) \\ f_{VNC}\left(xP^{l,t}\right) = \sum_{i=1}^{N} \left\langle \gamma_i^{l,t} - \gamma_i^* \right\rangle + \sum_{i=1}^{N} \left\langle I_i - \sum_{s=N+1}^{N+M} xP_s^{l,t} K_{s,i} \right\rangle \\ \qquad\qquad + \sum_{s=N+1}^{N+M} \left\langle \gamma_s^{l,t} - \gamma_s^* \right\rangle \end{cases} \tag{12}$$

$$l \in \{1, 2, \ldots, Sp\}, t \in \{0, 1, 2, \ldots, T\}$$

Where

$$\begin{cases} \gamma_i^{l,t} = \dfrac{xP_i^{l,t} G_{ii}}{\sigma_i + \sum_{i \neq j} xP_j^{l,t} G_{ji} + \sum_{s=N+1}^{N+M} xP_s^{l,t} K_{si}} \\ \gamma_s^{l,t} = \dfrac{xP_s^{l,t} G_{ss}}{\sigma_s + \sum_{s \neq v} xP_v^{l,t} G_{vs} + \sum_{i=1}^{N} xP_i^{l,t} K_{is}} \end{cases} \tag{13}$$

Sp is the size of population. T represents the maximum number of iterations in the algorithm.

Evaluate the performances of the particle are used to find the optimal solution by the above the fitness function. Therefore, the velocity and position are updated by comparing with before and after the value of the fitness function as follows

$$\begin{cases} vP_h^{l,t+1} = \omega \cdot vP_h^{l,t} + c_1 rand\left(pbset_h^{l,t} - xP_h^{l,t}\right) \\ \qquad\qquad + c_2 rand\left(gbset_h^t - xP_h^{l,t}\right) \qquad , h \in \{1, 2, \ldots, N+M\} \\ xP_h^{l,t+1} = xP_h^{l,t} + vP_h^{l,t+1} \end{cases} \tag{14}$$

Where

$$\omega = \omega_1 - \frac{(\omega_1 - \omega_2) \cdot t}{T} \tag{15}$$

$vP_h^{l,t}$ and $vP_h^{l,t+1}$ represent the hth dimension the velocity of the particle l in the tth and $(t+1)$th iteration, respectively. c_1 and c_2 are accelerated learning factors. $rand$ denotes the random number between 0 and 1. $xP_h^{l,t+1}$ represents the hth dimension the position of the particle l in the $(t+1)$th iteration. ω denotes an inertia weight coefficient, which can improve search accuracy with the increasing of the iteration time. ω_1 and ω_2 are maximum and minimum weight coefficients, respectively. $pbest_h^{l,t}$ denotes the hth dimension personal best position of the particle l in the tth iteration. $gbest_h^t$ denotes the hth dimension global best position in the tth iteration. The set of personal best position of the particle l in the tth iteration $pbest^{l,t} = \left[pbest_1^{l,t}, \ldots, pbest_h^{l,t}, \ldots, pbest_{M+N}^{l,t}\right]$ are described as follow

$$pbest^{l,t} = \begin{cases} xP^{l,t}, whent = 0 \\ xP^{l,t}, whent > 0, if F\left(xP^{l,t}\right) \succ F\left(pbest^{l,t-1}\right) \\ pbest^{l,t-1}, whent > 0, if F\left(pbest^{l,t-1}\right) \succ F\left(xP^{l,t}\right) \\ xP^{l,t}, whent > 0, if F\left(xP^{l,t}\right) \succ_n F\left(pbest^{l,t-1}\right) \end{cases} \tag{16}$$

Where $\succ$ denotes a dominated symbol. $\succ_n$ is a nondominated symbol. The judgment of dominant and nondominant relationship is shown in Table 1.

In order to obtain the global best solution, the nondominated archive is introduced to store the Pareto optimal solutions. According to the nondominated relation of the above table, the nondominated archive can be described as follows

$$Non^t = \begin{cases} \left[pbest^t\right], if t = 0 \\ \left[Non^{t-1} \cup pbest^t\right], if t > 0 \end{cases} \tag{17}$$

Where $pbest^t = \left[pbest^{1,t}, pbest^{2,t}, \ldots, pbest^{Sp,t}\right]$ is a set of personal best position in the tth iteration. Non^t represents the archive of the nondominated solutions in the tth iteration. $\lceil \bullet \rceil$ denotes a set of the nondominated solutions in $\bullet$.

Moreover, the above archive of the nondominated solutions is excessive to increase computation amount and reduce search performance of the algorithm. In order to manage Non^t and make distribution of the Pareto optimal solutions more uniform, it is necessary to reduce the size of the archive when the capacity of Non^t exceeds preset η. Therefore, the crowding distance is introduced as a performance index for management the archive, that is, the solutions of the crowding distance less than the average crowding distance are eliminated. The Non^t is managed as follows

$$\begin{aligned} Non^t = Non^t - Non^{\alpha,t}, \quad if\ CD^{\alpha,t} \leq \frac{\sum_{\delta=2}^{\beta-1} CD^{\delta,t}}{\beta - 1}, \\ \alpha \in \{2, 3, \ldots, \beta-1\} \text{ and } \beta > \eta \end{aligned} \tag{18}$$

Where $CD^{\delta,t}$ represent the crowding distance value of the Pareto optimal solution δ in the tth iteration. $Non^{\alpha,t}$ represents the Pareto optimal solution α from Non^t. $Non^t - Non^{\alpha,t}$ represents eliminating the Pareto optimal solution α from Non^t. β denotes the actual size of the archive Non^t.$CD^{\alpha,t}$ and $CD^{\delta,t}$ express the crowding distance value of the Pareto optimal solutions α and δ in the tth iteration, respectively. The calculation of the crowding distance is expressed below

$$CD^{\delta,t} = \begin{cases} \left|Non^{t,\delta,\max}\right| + \left|Non^{t,\delta,\min}\right|, \delta \in \{2, 3, \ldots, \beta-1\} \\ \infty, \delta \in \{1, \beta\} \end{cases} \tag{19}$$

where $Non^{t,\delta,\min}$ and $Non^{t,\delta,\max}$ denote the absolute values of small neighbor and large of the Pareto optimal solution δ in the tth iteration. In order to preserve the boundary solution, the crowding distance value of the boundary solution is set to $\delta \in \{1, \beta\}$.

After the management of (21), the selection of the Pareto optimal solution is easy to trap in local. Therefore, if the size of Non^t is still

Table 1
Determine the dominant relationship between $F\left(xP^{l,t}\right)$ and $F\left(pbest^{l,t-1}\right)$.

The dominant relation-ship between $F\left(xP^{l,t}\right)$ and $F\left(pbest^{l,t-1}\right)$	Number	The size relationship between $f_{Pu}\left(xP^{l,t}\right)$ and $f_{Pu}\left(pbest^{l,t-1}\right)$	The size relationship between $f_{Su}\left(xP^{l,t}\right)$ and $f_{Su}\left(pbest^{l,t-1}\right)$	The size relationship between $f_{VNC}\left(xP^{l,t}\right)$ and $f_{VNC}\left(pbest^{l,t-1}\right)$
$F\left(xP^{l,t}\right) \succ F\left(pbest^{l,t-1}\right)$	1	$f_{Pu}\left(xP^{l,t}\right) \geq f_{Pu}\left(pbest^{l,t-1}\right)$	$f_{Su}\left(xP^{l,t}\right) \geq f_{Su}\left(pbest^{l,t-1}\right)$	$f_{VNC}\left(xP^{l,t}\right) \leq f_{VNC}\left(pbest^{l,t-1}\right)$
$F\left(xP^{l,t}\right) \succ_n F\left(pbest^{l,t-1}\right)$	1	$f_{Pu}\left(xP^{l,t}\right) \geq f_{Pu}\left(pbest^{l,t-1}\right)$	$f_{Su}\left(xP^{l,t}\right) \geq f_{Su}\left(pbest^{l,t-1}\right)$	$f_{VNC}\left(xP^{l,t}\right) > f_{VNC}\left(pbest^{l,t-1}\right)$
	2	$f_{Pu}\left(xP^{l,t}\right) \geq f_{Pu}\left(pbest^{l,t-1}\right)$	$f_{Su}\left(xP^{l,t}\right) < f_{Su}\left(pbest^{l,t-1}\right)$	$f_{VNC}\left(xP^{l,t}\right) \leq f_{VNC}\left(pbest^{l,t-1}\right)$
	3	$f_{Pu}\left(xP^{l,t}\right) \geq f_{Pu}\left(pbest^{l,t-1}\right)$	$f_{Su}\left(xP^{l,t}\right) < f_{Su}\left(pbest^{l,t-1}\right)$	$f_{VNC}\left(xP^{l,t}\right) \leq f_{VNC}\left(pbest^{l,t-1}\right)$
	4	$f_{Pu}\left(xP^{l,t}\right) < f_{Pu}\left(pbest^{l,t-1}\right)$	$f_{Su}\left(xP^{l,t}\right) \geq f_{Su}\left(pbest^{l,t-1}\right)$	$f_{VNC}\left(xP^{l,t}\right) \leq f_{VNC}\left(pbest^{l,t-1}\right)$
	5	$f_{Pu}\left(xP^{l,t}\right) < f_{Pu}\left(pbest^{l,t-1}\right)$	$f_{Su}\left(xP^{l,t}\right) < f_{Su}\left(pbest^{l,t-1}\right)$	$f_{VNC}\left(xP^{l,t}\right) \leq f_{VNC}\left(pbest^{l,t-1}\right)$
	6	$f_{Pu}\left(xP^{l,t}\right) \geq f_{Pu}\left(pbest^{l,t-1}\right)$	$f_{Su}\left(xP^{l,t}\right) < f_{Su}\left(pbest^{l,t-1}\right)$	$f_{VNC}\left(xP^{l,t}\right) \leq f_{VNC}\left(pbest^{l,t-1}\right)$

greater than the preset η, the Non^t is processed again as follows

$$Non^t = Non^t - Non^{\arg\min CD^{\{2,\ldots,\beta-1\},t},t}, \quad if\ \beta > \eta \tag{20}$$

Where $Non^t - Non^{\arg\min CD^{\{2,\ldots,\beta-1\},t},t}$ denotes eliminating the Pareto optimal solutions with the smallest crowding distance from the Non^t. $\arg\min CD^{\{2,3,\ldots,\beta-1\}}$ represents sequence number of particle with the smallest crowding distance.

Then, the maximum crowding distance value of the Pareto optimal solutions is selected as the global best position in the above archive of the non-dominated solutions, which is different from random selection in the conventional MOPSO [23]. The proposed choice decreases the diversity of the population and increase the searching ability of the population on the Pareto front in this article. Therefore, the global best position is expressed as follows

$$gbest^t = Non^{\arg\max CD^{\{2,3,\ldots,\beta-1\},t},t} \tag{21}$$

Where $\arg\max CD^{\{2,3,\ldots,\beta-1\}}$ is sequence number of the Pareto optimal solutions with the greatest crowding distance value. $gbest^t$ denotes a set of the global best positions in the tth iteration.

Finally, in order to ensure that particle searches for the extreme values within the specified area and reduce the searching blindness, the position and velocity of particle on the hth dimension are restricted as follows

$$xP_h^{l,t} = \begin{cases} P_h^{\max}, if\, xP_h^{l,t} \geq P_h^{\max} \\ P_h^{\min}, if\, xP_h^{l,t} \leq P_h^{\min} \end{cases} \tag{22}$$

$$vP_h^{l,t} = \begin{cases} \left(P_h^{\max} - P_h^{\min}\right), if\, vP_h^{l,t} \geq \left(P_h^{\max} - P_h^{\min}\right) \\ -\left(P_h^{\max} - P_h^{\min}\right), if\, vP_h^{l,t} \leq -\left(P_h^{\max} - P_h^{\min}\right) \end{cases} \tag{23}$$

Where $P_h^{\min}, P_h^{\max}$ the minimum and maximum transmission power of user transmitter, respectively.

The summarization of the above transmit power control algorithm based on IMOPSO is below

Step 1.
Initialization:
set $K_{si} > 0$, $P_s > 0$, $I_i > 0$, $P_i > 0$, $G_{ii} = 1$, $G_{ij} > 0$, $\sigma_i > 0$, $P_j > 0$, $\gamma_i > 0$, $G_{ss} = 1$, $\sigma_s > 0$, $P_v > 0$, $G_{sv} > 0$, $\gamma_s > 0$, $K_{is} > 0$, $\gamma_i^* > 0$, $\gamma_s^* > 0$, $P_h^{\min} > 0$, $P_h^{\max} > 0$, $Sp > 0$, $T > 0$, $t = 0$, $P_h^{\min} \leq xP_h^{l,t} \leq P_h^{\max}$, $-\left(P_h^{\max} - P_h^{\min}\right) P_h^{\min} \leq vP_h^{l,t} \leq P_h^{\max} - P_h^{\min}$, $\omega_1 > 0$, $\omega_2 > 0$, $c_1 > 0$, $c_2 > 0$, $\eta > 0$.

Step 2. If $t > 0$, update the velocity and position of the particle by (14) and then $t = t + 1$, otherwise turn to **Step 3**.

Step 3. Calculate the fitness function by (12) and update the personal best position of particles by (16)

Step 4. Update the archive of nondominant solution by (17), (19) and (20).

Step 5. The global best position is selected in the archive of nondominant solution by (21)

Step 6. If $t <$ T, turn to **Step 2**. otherwise output archive of nondominant solution as optimal power control scheme.

3.2. Power control algorithm base on ICMOPSO

In order to enhance the diversity of the population and the searching ability on the boundary of Pareto front, an ICMOPSO algorithm is proposed to provide the diversified throughput distribution schemes for decision-making. According to the multi-population coevolutionary principle [24] and penalty theory [21], the model (8) is divided into two optimization schemes as follows

Scheme 1

$$\begin{aligned} &\max \sum_{i=1}^{N} \log\left(1 + r_i\right) \\ &\min \sum_{i=1}^{N} \left\langle \gamma_i - \gamma_i^* \right\rangle + \sum_{i=1}^{N} \left\langle I_i - \sum_{s=1}^{M} P_s K_{si} \right\rangle + \sum_{s=1}^{M} \left\langle \gamma_s - \gamma_s^* \right\rangle \\ &\text{s.t.} \begin{cases} 0 \leq P_i \leq P_i^{\max} \\ 0 \leq P_s \leq P_s^{\max} \end{cases} \end{aligned} \tag{24}$$

Scheme 2

$$\begin{aligned} &\max \sum_{s=N+1}^{N+M} \log\left(1 + r_s\right) \\ &\min \sum_{i=1}^{N} \left\langle \gamma_i - \gamma_i^* \right\rangle + \sum_{i=1}^{N} \left\langle I_i - \sum_{s=1}^{M} P_s K_{si} \right\rangle + \sum_{s=1}^{M} \left\langle \gamma_s - \gamma_s^* \right\rangle \\ &\text{s.t.} \begin{cases} 0 \leq P_i \leq P_i^{\max} \\ 0 \leq P_s \leq P_s^{\max} \end{cases} \end{aligned} \tag{25}$$

Where the first program is optimized the first population to maximize the concentration of the food A and minimize the concentration of the food C, and the second program is optimized the second population to maximize the concentration of the food B and minimize the concentration of the food C.

The fitness functions of the corresponding two schemes is rewritten as follows

The first population

$$F_u(P) = \begin{cases} f_{PU}(P) = \sum_{i=1}^{N} \log\left(1 + \gamma_i\right) \\ f_{VNC}(P) = \sum_{i=1}^{N} \left\langle \gamma_i - \gamma_i^* \right\rangle + \sum_{i=1}^{N} \left\langle I_i - \sum_{a=N+1}^{N+M} P_s K_{si} \right\rangle + \sum_{s=N+1}^{N+M} \left\langle \gamma_s - \gamma_s^* \right\rangle \end{cases}, \ if\ u = 1 \tag{26}$$

The second population

$$F_u(P) = \begin{cases} f_{SU}(P) = \sum_{s=N+1}^{N+M} \log\left(1 + \gamma_s\right) \\ f_{VNC}(P) = \sum_{i=1}^{N} \left\langle \gamma_i - \gamma_i^* \right\rangle + \sum_{i=1}^{N} \left\langle I_i - \sum_{s=N+1}^{N+M} P_s K_{si} \right\rangle + \sum_{s=N+1}^{N+M} \left\langle \gamma_s - \gamma_s^* \right\rangle \end{cases}, \ if\ u = 2 \tag{27}$$

Where $F_{u=1}(P)$ denotes the fitness function value and the food concentration of first population. $F_{u=2}(P)$ denotes the fitness function value and the food concentration of second population.

Accordingly, the position of the particle can be expressed below

$$\begin{aligned} xP^{L,t,u} &= \left(xP_1^{L,t,u}, \ldots, xP_h^{L,t,u}, \ldots, xP_{N+M}^{L,t,u}\right) \\ &= \left(xP_1^{L,t,u}, \ldots, xP_i^{L,t,u}, \ldots, xP_N^{L,t,u}, xP_{N+1}^{L,t,u}, \ldots, xP_s^{L,t,u}, \ldots, xP_{N+M}^{L,t,u}\right) \end{aligned} \tag{28}$$

Where $xP_h^{L,t,u}$ represents the hth dimension position of the particle L at the tth iteration of the uth ($u \in [1,2]$) population, and the transmitter transmission power of user on link h as well. $xP_i^{L,t,u}$ denotes the ith dimension position of the particle L in the tth iteration of the uth population, and the transmission power of PU-Tx on link i as well. $xP_s^{L,t,u}$ represents the sth dimension position of the particle L in the tth iteration of the uth population, and the transmission power of SU-Tx on link s as well. Therefore, the fitness function of the particle L in the tth iteration of the uth population is expressed as follows

$$\begin{aligned} &F_u\left(xP^{L,t,u}\right) \\ &= \begin{cases} f_{Pu}\left(xP^{L,t,u}\right) = \sum_{i=1}^{N} \log\left(1+\gamma_i^{L,t,u}\right) \\ f_{VNC}\left(xP^{L,t,u}\right) = \sum_{i=1}^{N} \left\langle \gamma_i^{L,t,u} - \gamma_i^* \right\rangle \\ \qquad + \sum_{i=1}^{N} \left\langle I_i - \sum_{s=N+1}^{N+M} xP_s^{L,t,u} K_{si} \right\rangle \\ \qquad + \sum_{s=N+1}^{N+M} \left\langle \gamma_s^{L,t,u} - \gamma_s^* \right\rangle \end{cases}, \ if\ u = 1 \\ &F_u\left(xP^{L,t,u}\right) \\ &= \begin{cases} f_{Su}\left(xP^{L,t,u}\right) = \sum_{s=N+1}^{N+M} \log\left(1+\gamma_s^{L,t,u}\right) \\ f_{VNC}\left(xP^{L,t,u}\right) = \sum_{i=1}^{N} \left\langle \gamma_i^{L,t,u} - \gamma_i^* \right\rangle \\ \qquad + \sum_{i=1}^{N} \left\langle I_i - \sum_{s=N+1}^{N+M} xP_s^{L,t,u} K_{si} \right\rangle \\ \qquad + \sum_{s=N+1}^{N+M} \left\langle \gamma_s^{L,t,u} - \gamma_s^* \right\rangle \end{cases}, \ if\ u = 2 \\ &L \in \left\{1, 2, \ldots, \frac{Sp}{2}\right\} \end{aligned} \tag{29}$$

Where

$$\begin{cases} \gamma_i^{L,t,u} = \dfrac{xP_i^{L,t,u} G_{ii}}{\sigma_i + \sum_{i \neq j} xP_j^{L,t,u} G_{ji} + \sum_{s=N+1}^{N+M} xP_s^{L,t,u} K_{si}} \\ \gamma_s^{L,t,u} = \dfrac{xP_s^{L,t,u} G_{ss}}{\sigma_s + \sum_{s \neq v} xP_v^{L,t,u} G_{vs} + \sum_{i=1}^{N} xP_i^{L,t,u} K_{is}} \end{cases} \tag{30}$$

In order to find the optimal solution by the above the fitness function, the velocity and position is updated as follows

$$\begin{cases} vP_h^{L,t+1,u} = \omega^t \cdot vP_h^{L,t,u} + c_1 rand\left(pbset_h^{L,t,u} - xP_h^{L,t,u}\right) \\ \qquad\qquad + c_2 rand\left(gbset_h^{t,u} - xP_h^{L,t,u}\right) + c_3 rand\left(Archive_h^{L,t,u} - xP_h^{L,t,u}\right) \\ xP_h^{L,t+1,u} = xP_h^{L,t,u} + vP_h^{L,t+1,u} \end{cases} \tag{31}$$

Where $vP_h^{L,t,u}$ is the hth dimensional velocity of particle L in the tth iteration of the uth population. $pbest_h^{L,t,u}$ denotes the hth dimensional personal best position of particle L in the tth iteration of the uth population. $gbest_h^{t,u}$ represent the hth dimensional global best position of particle L in the tth iteration of the uth population. c_3 is accelerated learning factor. $Archive_h^{L,t,u}$ denotes the hth dimensional archives information of particle L in the tth iteration of the uth population. The information is shared to accelerate learning other particles between different populations by external archive, namely $c_3 rand\left(Archive_h^{L,t,u} - xP_h^{L,t,u}\right)$.

The set of personal best position $pbest^{L,t,u} = \left[pbest_1^{L,t,u}, \ldots, pbest_h^{L,t,u}, \ldots, pbest_{N+M}^{L,t,u}\right]$ is rewritten as follows

$$pbest^{L,t,u} = \begin{cases} xP^{L,t,u}, whent = 0 \\ xP^{L,t,u}, whent > 0, if\ F_u\left(xP^{L,t,u}\right) \succ F_u\left(pbest^{L,t-1,u}\right) \\ pbest^{L,t-1,u}, whent > 0, if\ F_u\left(pbest^{L,t-1,u}\right) \succ F_u\left(xP^{L,t,u}\right) \\ xP^{L,t,u}, whent > 0, if\ F_u\left(xP^{L,t,u}\right) \succ_n F_u\left(pbest^{L,t-1,u}\right) \end{cases} \tag{32}$$

The global best position is selected randomly in the set of nondomination solutions, which is in the scope of the personal best positions' set. That can be described as follows

$$gbest^{t,u} = random\left(\left[pbest^{t,u}\right]\right) \tag{33}$$

Where $gbest^{t,u} = \left[gbest_1^{t,u}, \ldots, gbest_h^{t,u}, \ldots, gbest_{N+M}^{t,u}\right]$ is a global best position in the tth iteration of the uth population. $pbest^{t,u} = \left[pbest^{1,t,u}, pbest^{2,t,u}, \ldots, pbest^{\frac{Sp}{2},t,u}\right]$ represents the set of the personal best positions. $random(\bullet)$ denotes the solution which is randomly selected from the set of $\bullet$.

To strengthen collaboration between the different populations and quickly approach to the true Pareto front, the position of the archive is defined as follows

$$Archive^{L,t,u} = \begin{cases} gbest^{t,2}, \ if\ EA^t = \varnothing\ and\ \mathrm{u} = 1 \\ gbest^{t,1}, \ if\ EA^t = \varnothing\ and\ \mathrm{u} = 2 \\ random\left(Non^t\right), \ if\ EA^t \neq \varnothing \end{cases} \tag{34}$$

Where $Archive^{L,t,u}$ denotes the position of the archive solution L in the tth iteration of the uth population. EA^t represents the external archive in the tth iteration, which stores the Pareto optimal solutions from all the populations, namely the optimal power control scheme in the tth iteration. Therefore, EA^t is expressed as follows

$$EA^t = \begin{cases} \left[pbest^{t,1} \cup pbest^{t,2}\right], \ if\ t = 0 \\ \left[pbest^{t,1} \cup pbest^{t,2} \cup Non^{t-1}\right], \ if\ t > 0 \end{cases} \tag{35}$$

Where $pbest^{t,1}$ and $pbest^{t,2}$ denotes the set of personal best position in the first and the second population, respectively. The above domination relationship of (35) is determined by (10).

In order to enhance the diversity of population, the Gauss perturbation strategy [25] of the single dimension is introduced to process EA^t. It can be expressed as follows

$$Nop_d^{\alpha,t} = EA_d^{\alpha,t} + \left(P_d^{\max} - P_d^{\min}\right) \cdot Gaussian(0,1) \tag{36}$$

Where d is the random dimension ($d \in \{1, 2, \ldots, N+M\}$). $EA_d^{\alpha,t}$ denotes the dth dimension position of the solution α in the tth iteration of the external archive. $Nop_d^{\alpha,t}$ represents the position of $EA_d^{\alpha,t}$ by the Gauss perturbation. The nondominant solutions of $Nop^t = \begin{bmatrix} Nop_1^{1,t}, Nop_2^{1,t}, \ldots, Nop_{N+M}^{1,t} \\ Nop_1^{2,t}, Nop_2^{2,t}, \ldots, Nop_{N+M}^{2,t} \\ \vdots \quad \ddots \quad \vdots \\ Nop_1^{\beta,t}, Nop_2^{\beta,t}, \ldots, Nop_{N+M}^{\beta,t} \end{bmatrix}$ is stored to EA^t, namely $EA^t = \left[Nop^t\right]$. Similarly, in order to obtain a uniformly distributed set of Pareto optimal solution, the external archive is reduced by (21) and (22), until the actual size of the external archive β is not exceed the maximum capacity η.

According to constraints $C4$ and $C5$ of model (9), the limitation of particle's velocity and position is similar to avoid blind searching in the MOPSO algorithm. It can be expressed below

$$vP_h^{L,t,u} = \begin{cases} P_h^{\max}, if\, vP_h^{L,t,u} \geq P_h^{\max} \\ P_h^{\min}, if\, vP_h^{L,t,u} \leq P_h^{\min} \end{cases} \tag{37}$$

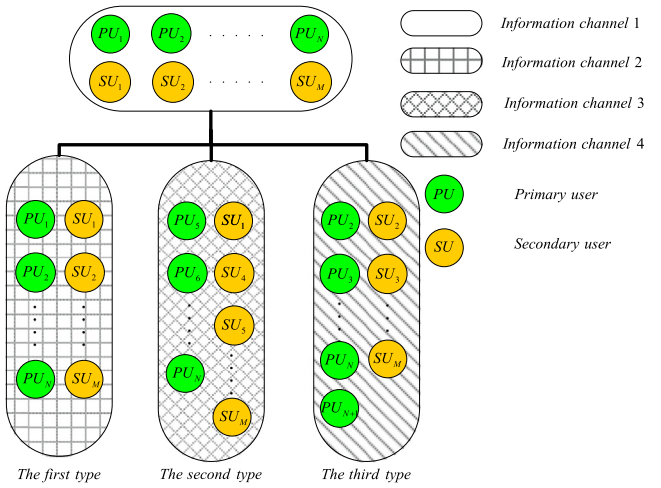

Fig. 2. Three types of dynamic communication environment.

$$xP_h^{L,t,u} = \begin{cases} P_h^{\max}, if\, xP_h^{L,t,u} \geq P_h^{\max} \\ P_h^{\min}, if\, xP_h^{L,t,u} \leq P_h^{\min} \end{cases} \tag{38}$$

The summarization of the above transmit power control algorithm based on ICMOPSO is

Step 1. Initialization: set $K_{si} > 0$, $P_s > 0$, $I_i > 0$, $P_i > 0$, $G_{ii} = 1$, $G_{ij} > 0$, $\sigma_i > 0$, $P_j > 0$, $\gamma_i > 0$, $G_{ss} = 1$, $\sigma_s > 0$, $P_v > 0$, $G_{sv} > 0$, $\gamma_s > 0$, $K_{is} > 0$, $\gamma_i^* > 0$, $\gamma_s^* > 0$, $P_h^{\min} > 0$, $P_h^{\max} > 0$, $Sp > 0$, $T > 0$, $t = 0$, $P_h^{\min} \leq xP_h^{l,t,u} \leq P_h^{\max}$, $-\left(P_h^{\max} - P_h^{\min}\right) P_h^{\min} \leq vP_h^{l,t,u} \leq P_h^{\max} - P_h^{\min}$, $\omega_1 > 0$, $\omega_2 > 0$, $c_1 > 0$, $c_2 > 0$, $c_3 > 0$, $\eta > 0$.

Step 2. If $t > 0$, update the velocity and position of the particle according to Eq. (32). Then, let $t = t + 1$, otherwise turn to **Step 3**.

Step 3. Calculate the fitness function by (30)

Step 4. Judge the relationship of dominance and update the personal best positions by (32)

Step 5. Update the global best positions by (33)

Step 6. Update the external archive by (22), (23), (35) and (36).

Step 7. The archive position is selected from external archive or global best positions by (34)

Step 8. If $t <$ T, return to **Step 2.** otherwise output external archive as optimal power control scheme.

3.3. Dynamic response strategy of power control algorithm in dynamic environment

In this section, considered the real time change of channel parameters and users' working status in CRNs, the continuously changeable communication environment is divided into three major types in Fig. 2, where **the first type is** the unchangeable number of user and changeable channel parameters. **The second type** is no new users joining in, the decreasing number of users and the channel parameters. **The third type** is new users joining in, and both the changeable channel parameters and number of users.

In order to better solve the above dynamic problem, the corresponding dynamic response strategies is proposed to improve the convergence rate based on ICMOPSO algorithm as shown in Table 2. Furthermore, the communication status of users is provided by the sensor and the changes of channel is monitored by the sentinel particles. However, the disadvantage of the sentinel particle is insufficient for the solution space. Therefore, the nondominated solutions in the tth iteration of external archive $EA^{t-1,y}$ on the yth environment is taken as the sentinel particles, which monitor the changeable degrees $Eci^{t,y}$ in the tth iteration on the yth environment. It can be depicted as

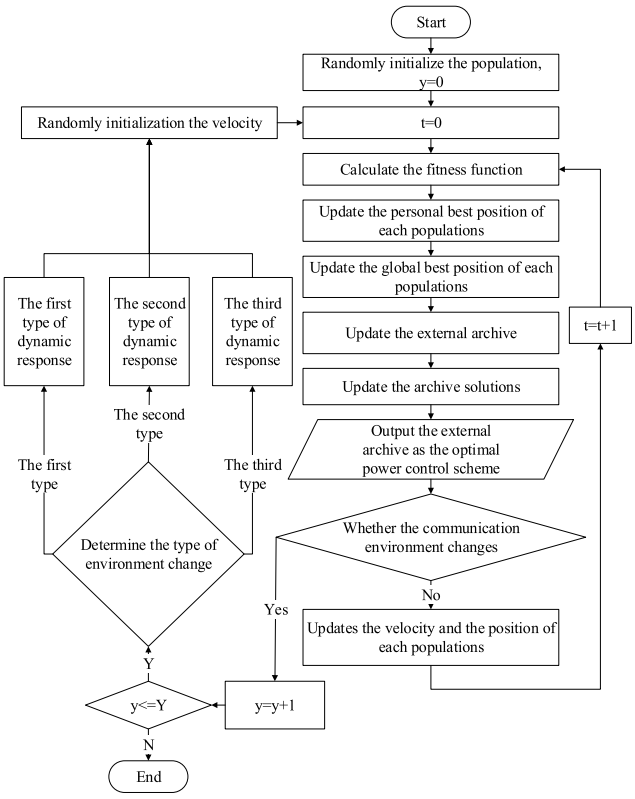

Fig. 3. Flow chart of dynamic power control algorithm base on ICMOPSO.

$$Eci^{t,y} = \sum_{\alpha=1}^{\beta} \left| F\left(EA^{\alpha,t-1,y}\right)^t - F\left(EA^{\alpha,t-1,y}\right)^{t-1} \right| \tag{39}$$

Where $F\left(EA^{\alpha,t-1,y}\right)^t$ and $F\left(EA^{\alpha,t-1,y}\right)^{t-1}$ represent the food concentration of the solution α of $EA^{t-1,y}$ in the tth and $(t-1)$th iteration on the yth environment.

If $Eci^{t,y}$ is not more than the changeable degrees threshold of environment Eci^*, the position and the velocity of particles as well as the external archive is also unchangeable. It can be equivalently written as

$$\begin{aligned} xP^{t,u,y} &= xP^{t-1,u,y} \\ vP^{t,u,y} &= vP^{t-1,u,y} \\ EA^{t,y} &= EA^{t-1,y} \end{aligned} \tag{40}$$

If $Eci^{t,y}$ is greater than the changeable degrees threshold of environment Eci^*, the communication environment has changed in the tth iteration. Specific expressions are detailed in Table 2.

In order to avoid falling into the local optimization, the velocity of particles is reinitialized in new communication environment as follows

$$vP_h^{L,t=0,u,y+1} = rand\left(vP_h^{\min}, vP_h^{\max}\right) \tag{41}$$

Where $vP_h^{L,t=0,u,y+1}$ denotes the hth dimension velocity of particle L in the $(t=0)$th iteration of the uth population on the $(y+1)$th environment. $rand\left(vP_h^{\min}, vP_h^{\max}\right)$ represent the value of the random initialization between $vP_h^{\min}$ and $vP_h^{\max}$.

Finally, the flow chart of ICMOPSO algorithm for power control in changeable environment is expressed in Fig. 3.

Table 2
Dynamic response strategy.

	Implementation process of strategies
The first type of environment	If $Eci^{t,y} > Eci^{*}$ holds, $EA^{t-1,y}$ and random initialization of 200 particles are stored in the $EA^{t=0,y+1}$ on the $y+1$ thenvironment. Moreover, in each of population, the positions of 30% particles are reinitialized and that of 10% particles are treatment of variation in the y thenvironment. Therefore, the positions of the particles $xP^{t=0,u,y+1}$ are changeable in the $(y+1)$ thenvironment as follow $xP^{t=0,u,y+1} = xP^{Initialize(30\%),t-1,u,y} \cup xP^{Muation(10\%),t-1,u,y} \cup xP^{Original(60\%),t-1,u,y}$ (42) Where $xP_d^{Muation(30\%),t-1,u,y} = rand\left(xP_d^{\min}, xP_d^{\max}\right)$ (43) $xP^{Initialize(30\%),t-1,u,y}$ is the positions of reinitialized 30% particles in the $(t-1)$ thiteration of the u thpopulation on the y thenvironment. $xP^{Muation(10\%),t-1,u,y}$ denotes the positions of reinitialized 10% particles by treatment of single dimension variation in the $(t-1)$ thiteration of the u th population on the y thenvironment. $xP^{Original(60\%),t-1,u,y}$ represents the positions of 60% original particles in the $(t-1)$ thiteration of the u thpopulation on the y thenvironment. d is the random dimension $(d \in \{1,2,\ldots,N+M\})$.
The second type of environment	When the user h leaves the communication network, the dimension information of the corresponding particle is removed namely $xP^{t-1,u,y} = \left(xP_1^{t-1,u,y}, xP_2^{t-1,u,y}, \ldots, xP_{h-1}^{t-1,u,y}, xP_{h+1}^{t-1,u,y}, \ldots, xP_{N+M}^{t-1,u,y}\right)$. Similarly, the external archive is also handled $EA^{t=0,y+1} = \left(EA_1^{t-1,y}, EA_2^{t-1,y}, \ldots, EA_{h-1}^{t-1,y}, EA_{h+1}^{t-1,y}, \ldots, EA_{N+M}^{t-1,y}\right)$ and random initialization of 200 particles is stored in the $EA^{t=0,y+1}$. After the above of treatment, 30% particles of the u thpopulation are reinitialized to obtain the $xP^{Initialize(30\%),t-1,u,y}$, and 20% particles of the u thpopulation are treated with a single dimension variation to obtain $xP^{Muation(20\%),t-1,u,y}$. Finally, the set of the particles in the $(t=0)$ thiteration of the u thpopulation on the $(y+1)$ th environment is as follows $xP^{t=0,u,y+1} = xP^{Initialize(30\%),t-1,u,y} \cup xP^{Muation(20\%),t-1,u,y} \cup xP^{Original(50\%),t-1,u,y}$ (44) where, $xP^{Original(50\%),t-1,u,y}$ represents the 50% original particles in the $(t-1)$ thiteration of the u thpopulation on the y thenvironment.
The third type of environment	When a new user enters the communication network, we define a new dimension to the original particle in the population, namely $xP^{t-1,u,y} = \left(xP_1^{t-1,u,y}, xP_2^{t-1,u,y}, \ldots, xP_{N+M}^{t-1,u,y}, xP_{N+M+1}^{t-1,u,y}\right)$. $xP_{N+M+1}^{t-1,u,y}$ is the particle position of the $(N+M+1)$ th dimension of the u thpopulation on the y thenvironment, it is randomly initialized within the range of values. When the user h leaves the communication network, the dimension information of the correspond particle is removed, namely $xP^{t-1,u,y} = \left(xP_1^{t-1,u,y}, xP_2^{t-1,u,y}, \ldots, xP_{h-1}^{t-1,u,y}, xP_{h+1}^{t-1,u,y}, \ldots, xP_{N+M}^{t-1,u,y}\right)$. After the above of treatment, 50% particles of the u thpopulation are reinitialized to obtain the $xP^{Initialize(50\%),t-1,u,y}$, and 10% particles are treated with a single dimension variation to obtain $xP^{Muation(10\%),t-1,u,y}$. Finally, the collection of the particles in the $(t=0)$ thiteration of the u thpopulation on the $(y+1)$ thenvironment is as follows $xP^{t=0,u,y+1} = xP^{Initialize(50\%),t-1,u,y} \cup xP^{Muation(10\%),t-1,u,y} \cup xP^{Original(40\%),t-1,u,y}$ where $xP^{Original(40\%),t-1,u,y}$ (45) where $xP^{Original(40\%),t-1,u,y}$ represents the 40% particles in the $(t-1)$ thiteration of the u thpopulation on the y thenvironment. Moreover, random initialization of 200 particles is stored in the $EA^{t=0,y+1}$.

4. Simulation

In this section, computer simulations demonstrate the theoretical discussions and results of the previous sections in the above. Specifically, two proposed schemes based on IMOPSO and ICMOPSO can obtain the maximum throughput of PUs' and SUs' and guarantee the QoS of the PUs and SUs. Moreover, we can conclude that ICMOPSO algorithm obtain the best scheme of diversity and ability of searching through comparing the performance of ICMOPSO with that of IMOPSO, IMOCPSO [26] and IMOQPSO [27] algorithm. Finally, in the environment of dynamic communication, the performances of the three dynamic response strategies based on ICMOPSO algorithm are better than that of the static strategies.

In the underlay cognitive radio network, we assume there are the transmitter–receiver pairs of four PUs and the transmitter–receiver pairs of four SUs. The parameters of cognitive radio and power control algorithm are shown in following Tables 3 and 4.

From Fig. 4, it is obviously that the performances of the ICMOPSO algorithm are superior to that of IMOPSO. Specifically, the throughput [2.8, 5.4] of PUs in the ICMOPSO algorithm in has the better searching ability of boundary and than that [3.9, 5.3] of in IMOPSO. Meantime, ICMOPSO algorithm can get the more wider distribution schemes for the throughput [2.8, 3.9] [5.3, 5.4] of PUs and SUs than IMOPSO. And ICMOPSO algorithm is superior to the IMOPSO algorithm on the true Pareto front.

From Fig. 5, the received interference from each PU is always less than 0.25 in 20 group power allocation schemes, which indicates that the constraints of $C1$ is satisfied with IMOPSO and ICMOPSO. However, a phenomenon is found that is number of schemes and lines based on IMOPSO and ICMOPSO algorithms. Because several identical solutions exist in the total of interferences generated from all SU-Txs to PU-Rx.

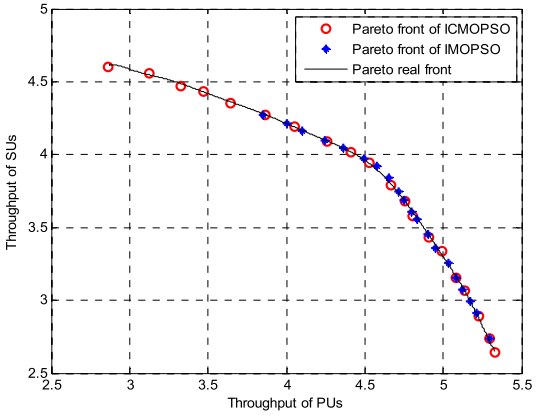

Fig. 4. Pareto front of throughput of PUs and SUs(a) IMOPSO (b) ICMOPSO.

From Fig. 6, the SINR of PU is always greater than 1db, and the SINR of SU is always more than 0.8 db. The minimum SINR constraints of PU ($C2$) and SU ($C3$) are satisfied in two proposed algorithms, which can ensure QoS for SUs and PUs. Meantime, the number of schemes is also in-consistent with that of lines for several identical solutions.

In the actual communications, the transmission power of the user is normally limited due to its own device factors. What shows in Fig. 7 is the 20 group power allocation schemes corresponding to 20 throughput optimal allocation schemes, which the transmission power of each SU's and PU's transmitter is below the maximum permitted transmit power of each transmitter (1 mw) in thermal maps. Therefore, the system constraints $C4$ and $C5$ are satisfied in IMOPSO and ICMOPSO.

Table 3
Cognitive radio system information.

Meaning	Symbol	Value range
Transmission power of the PU-Tx at link i	P_i (mW)	[0.1, 1]
Transmission power of the SU-Tx at link s	P_s (mW)	[0.1, 1]
Direct channel gain from the PU-Tx to the PU-Rx at link i	G_{ii}	1
Interference gain from the PU-Tx at link $i$to the PU-Rx at link j	G_{ij}	[0.1, 1]
Direct channel gain from the SU-Tx to SU-Rx at the link s	G_{ss}	1
Interference gain from the SU-Tx on link $s$to the SU-Rx on link v	G_{sv}	[0, 0.15]
Interference gain from the PU-Tx on link $i$to the SU-Rx on link s	K_{is}	[0.1, 1]
Interference gain from the SU-Tx on link $s$to the PU-Rx on link i	K_{si}	[0, 0.15]
Interference threshold of the PU-Rx on link i	I_i	0.25
SINR threshold of the PU-Rx on link i	γ_i^* (dB)	1
SINR threshold of the SU-Rx on link s	γ_s^* (dB)	0.8
Background noise power of the PU-Rx on link i	σ_i (mW)	[0, 0.01]
Background noise power of the SU-Rx on link s	σ_s (mW)	[0, 0.015]

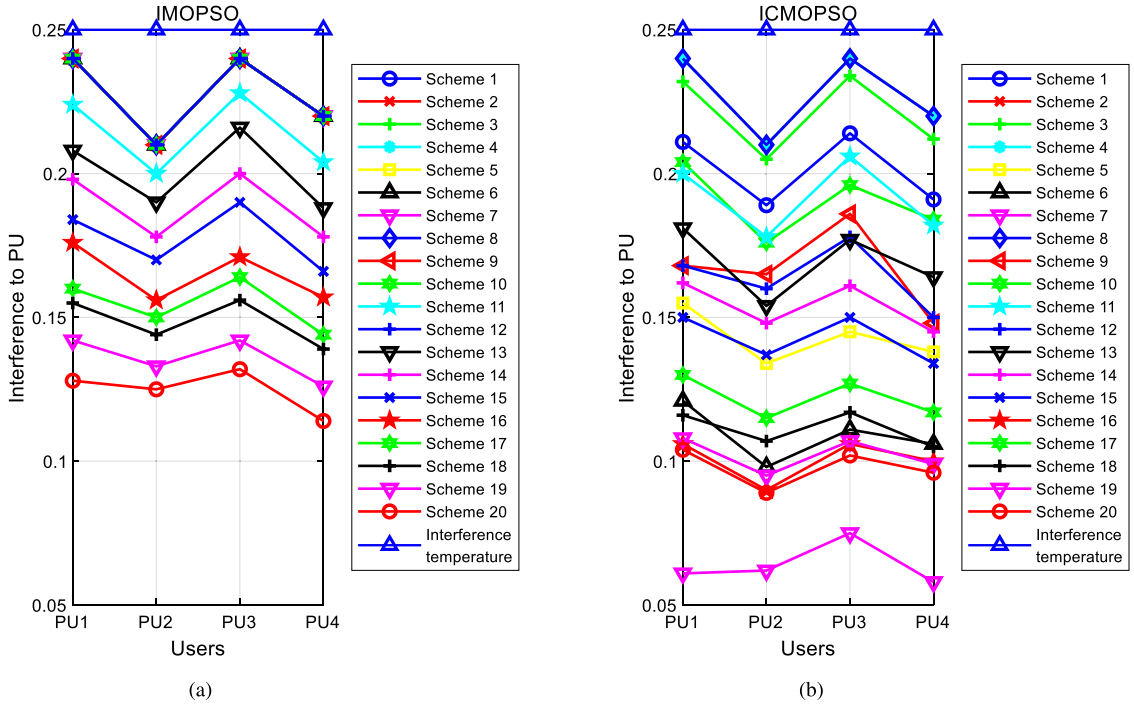

Fig. 5. Interference to every PU (a) IMOPSO (b) ICMOPSO.

In order to evaluate the above cognitive radio system, CV, GD and MS were compared by 100 sets of the throughput on Pareto front based on MOPSO and IMOPSO, CMOPSO and ICMOPSO, multi-objective chaotic particle swarm (MOCPSO) and IMOCPSO, multi-objective quantum particle swarm (MOQPSO) and IMOQPSO in Figs. 8–10.

According to the definition of the CV, when the CV is getting smaller, the distribution scheme for throughput of PUs and SUs is going to be more uniform. As shown in Fig. 8, it is obviously that the scheme of the throughput of PUs and SUs of IMOPSO, ICMOPSO, IMOCPSO and IMOQPSO algorithm is better than that of MOPSO, CMOPSO, MOCPSO [26] and MOQPSO [27] algorithm based on improved crowding distance archive management from (a), (b), (c) and (d) respectively. Furthermore, in order to obtain the optimal distribution scheme of the throughput of PUs and SUs, it is compared with the CV in IMOPSO, ICMOPSO, IMOCPSO and IMOQPSO algorithms from Fig. 8 (e). It can be shown that CV of ICMOPSO algorithm is significantly better than the other three algorithms and the optimal distribution scheme of the throughput of PUs and SUs is obtained by ICMOPSO.

According to the definition of the GD, when the smaller GD is, the smaller error between Pareto front and the real frontier is, namely the throughput allocation scheme is closer to the real optimal. Fig. 9 shows that the performances of IMOPSO and ICMOPSO are significantly better than other algorithms. Furthermore, it can be known that the median of GD is 0.00408884, maximum value is 0.00859784 and the minimum value is 0.00142396 in ICMOPSO algorithm, which is smaller than that of IMOPSO algorithm by analyzing Table 5. Moreover, the uncertainty of ICMOPSO algorithm is much less than that of IMOPSO algorithm.

The larger the known index MS is, the better the algorithm can explore the boundary of the real Pareto front, which means that more diversified throughput schemes can be provided for the decision maker.

Table 4
Information for algorithm.

Meaning	Symbol	Value range
Maximum flight speed of particles	$V_{\max}$	1
Minimum flight speed of particles	$V_{\min}$	−1
The largest population (MOPSO, MOCPSO and MOQPSO)	Sp_1	300
Maximum capacity of each population (CMOPSO)	$\frac{Sp}{2}$	150
Maximum iterations	T	100
Nondominated archives maximum capacity	η	20
Maximum weight	ω_1	0.9
Minimum weight	ω_2	0.4
Learning factor	c_1, c_2, c_3	1.4495
Minimum weight	ω_2	0.4
Determine the threshold of environmental change	Eci^*	10^{-2}

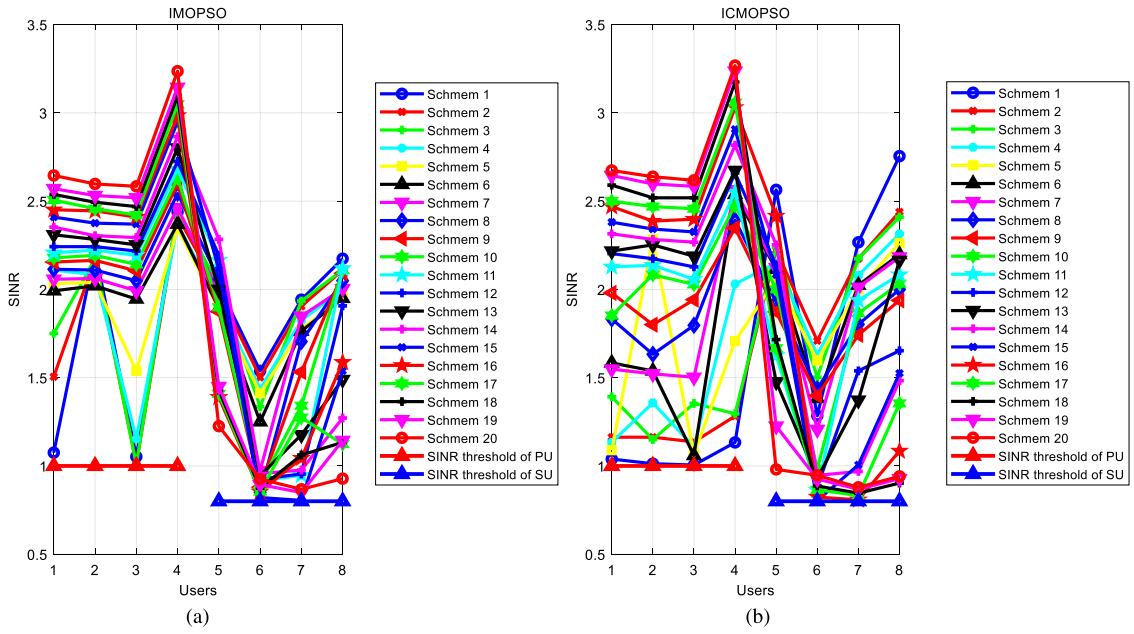

Fig. 6. The SINR of every user (a) IMOPSO (b) ICMOPSO.

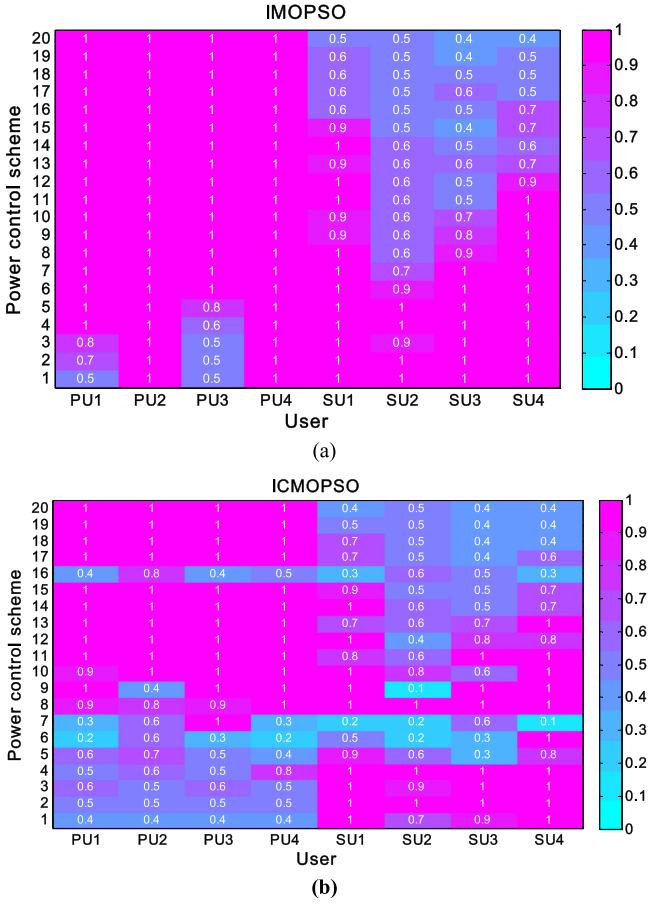

Fig. 7. The transmission power of PU-Txs and SU-Txs. (a) IMOPSO (b) ICMOPSO. ("1" represents the maximum permitted transmit power of each transmitter in Fig. 7.)

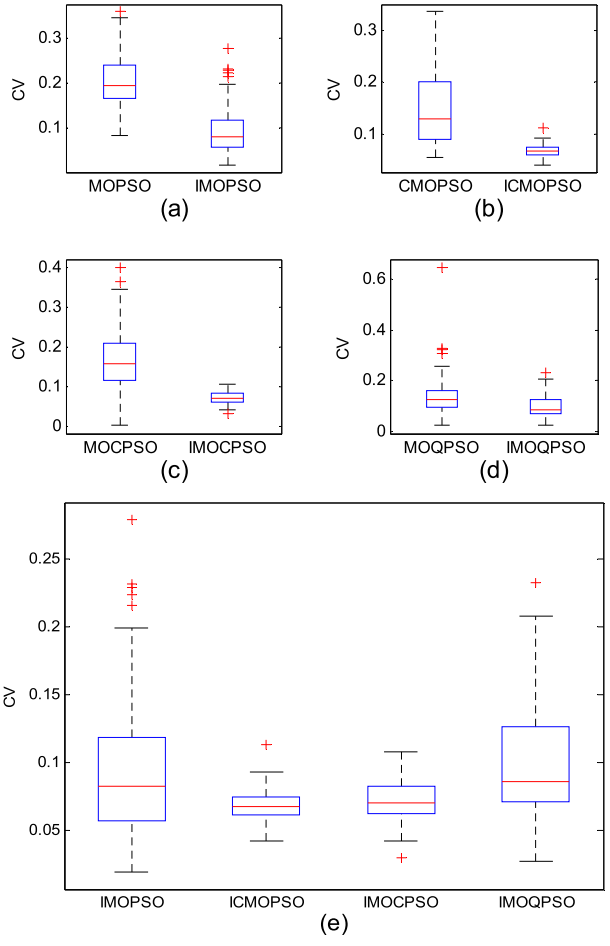

Fig. 8. Comparison of CV (a) MOPSO and IMOPSO (e) the four improved algorithms.

According to the data in Fig. 10, we can see that MS of the ICMOPSO algorithm is obviously better than other algorithms.

In conclusion, through comprehensive comparing the performance indexes of CV, GD and MS, the performance of ICMOPSO algorithm is

Table 5
Comparison of GD in IMOPSO and ICMOPSO.

	Median	Maximum	Minimum	Num Points	Num Finite Outliers
IMOPSO	0.00715508	0.02058769	0.00157372	50	2
ICMOPSO	0.00408884	0.00859784	0.00142396	50	0

Table 6
The changeable user's information in 20 dynamic environments.

	Channel	PU1	PU2	PU3	PU4	PU5	PU6	PU7	PU8	SU1	SU2	SU3	SU4	SU5	SU6	SU7	SU8
Initial		■	■	■		■					■	■		■			■
1	√	■	■	■		■					■	■		■			■
2	√		■	■		■					■	■		■			■
3	√				■	■	■			■	■	■		■			
4	√		■		■	■	■			■	■	■		■			
5	√		■		■	■	■				■	■		■			
6	√				■	■	■				■	■		■			
7	√	■	■				■	■		■	■						■
8	√		■			■	■		■		■		■	■			
9	√					■	■		■		■		■	■			
10	√	■	■			■			■		■		■			■	
11	√	■	■			■			■		■		■			■	
12	√				■	■			■				■	■	■		
13	√	■			■	■		■		■			■			■	■
14	√	■			■	■		■		■			■			■	■
15	√	■	■		■		■						■		■	■	
16	√		■				■						■		■	■	
17	√		■	■			■				■	■	■				■
18	√		■	■			■				■	■	■				■
19	√		■	■			■				■	■					■
20	√	■	■	■					■		■	■	■				■

✓ represents the change of channel parameter, ■ represents the occupancy of user communication.

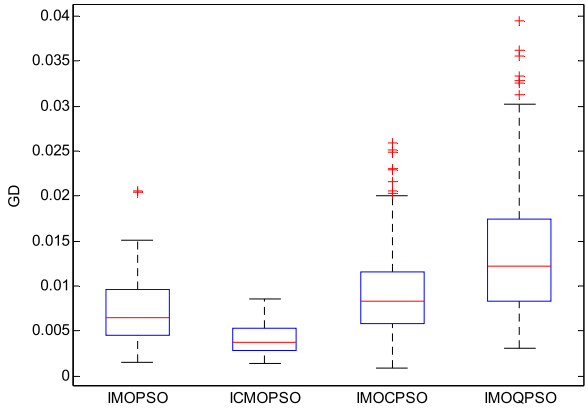

Fig. 9. Comparison of GD of the four algorithms.

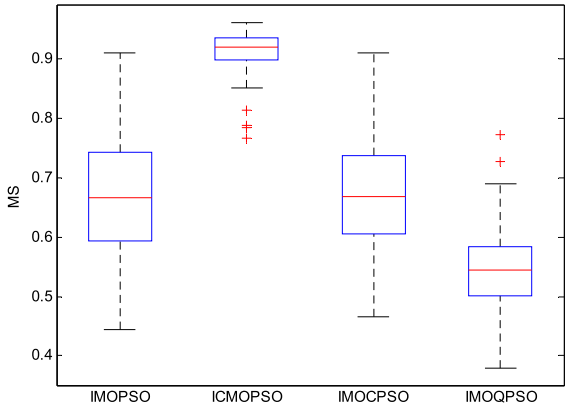

Fig. 10. Comparison of MS in the four algorithms.

more superior to the other algorithms in static communication scenarios. In additional, a certain number of static communication scenarios can be obtained by sampling the dynamic communication environment. So, we can draw the conclusion that this ICMOPSO algorithm is also superior to the other algorithms in dynamic environment. Therefore, the dynamic and static strategies based on ICMOPSO are further only analyzed and discussed in the dynamic communication environment. Meantime, the validity of the conclusion in Fig. 4 is verified by the index data of CV, GD and MS.

In a real communication system, the channel and the number of users are randomly changeable. Thus, changeable communication environment is divided into the three types in Table 6. It shows that the results of user communication status and changeable channel parameters in 20 dynamic environments, which the first and second types of dynamic environments account for 25%, and the third dynamic environment account for 50%.

In order to evaluate the dynamic response strategy, an ideal static response strategy is introduced by initializing the population after the change of communication environment. In addition, the parameters of system in cognitive radio network and algorithm ICMOPSO in cognitive radio system are still the same as those in Tables 3 and 4. Therefore, in the same iterations of ICMOPSO algorithm, we should compare with the above performances of CV, GD, MS and the maximum number iterations of the CT (CV < 0.1, GD < 0.001 and MS > 0.9) on static and dynamic response strategy.

The performances of CV, GD, MS and the maximum number iterations of the CT (CV < 0.1, GD < 0.001 and MS > 0.9) are shown in Fig. 11(a), (b), (c), (d), which describes the dynamic and static strategy in three types of dynamic communication environments. From the comparison of IMOPSO and ICMOPSO, we know that the smaller CV, GD and CT, the larger MS, the better performance of the algorithm. The MS value of the dynamic strategy is better than that of the static strategy in Fig. 11(b); Fig. 11 (**d**) shows that The CT value of the dynamic strategy is lower than that of the static strategy at a lower computational cost. According to the above theory, these two values of the dynamic strategy is better than that of the static strategy. However, in Fig. 11(a), (c), there is little difference between CV and GD in

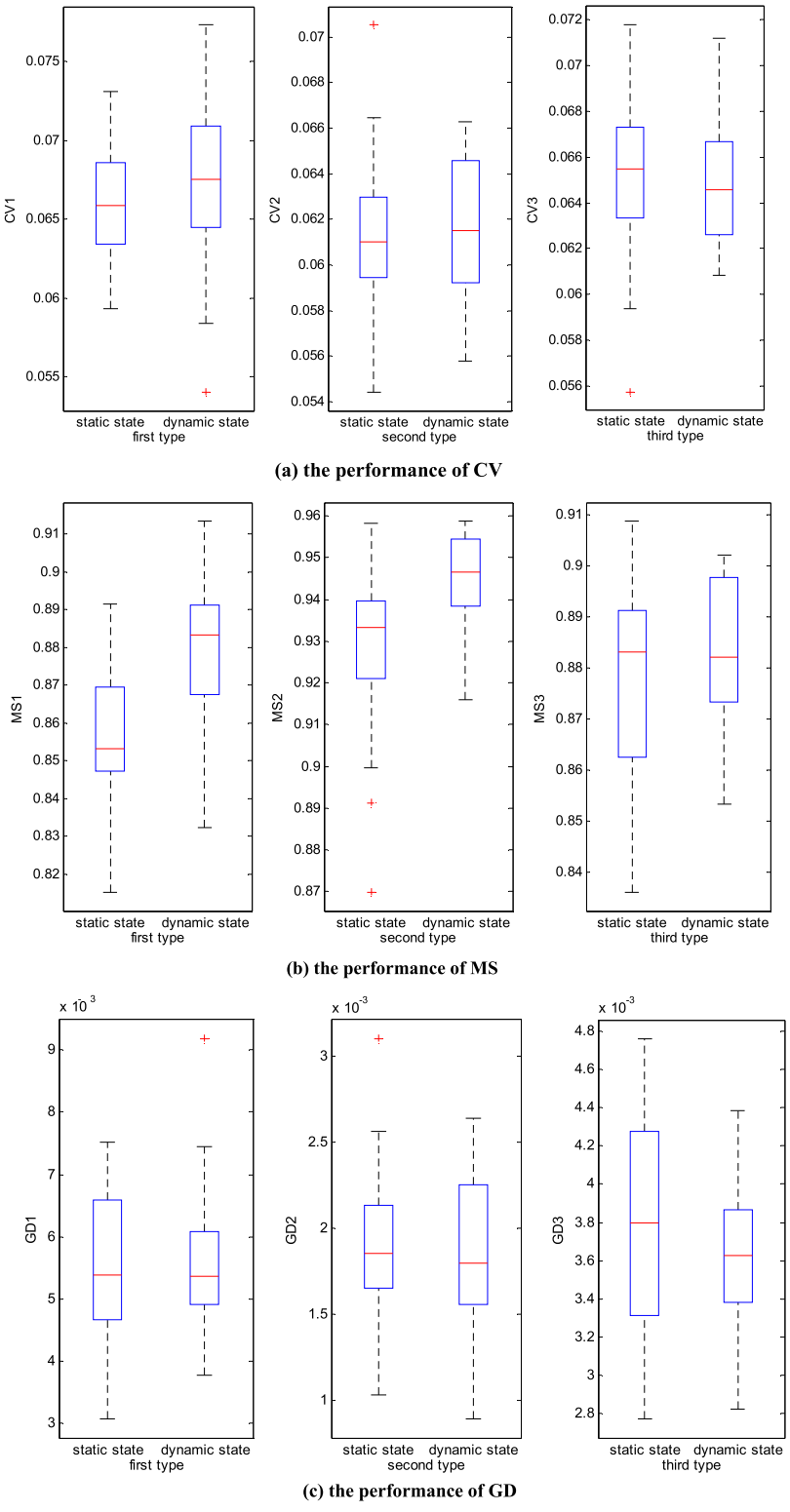

Fig. 11. Performances of the dynamic and static response strategies in three types of environments.

dynamic and static strategies for three types of dynamic communication environments. Especially, the CV1 and GD1 of the dynamic strategy are unexpectedly inferior to that of the static strategy in Table 7. The fundamental reason is that compared with MS2-3 in Fig. 11(b), the maximum search range of dynamic strategy in MS1 is much wider than that of static strategy, which leads to the performance degradation of CV1 and GD1. Furthermore, the overall performance of the dynamic and static strategy is described by the CV4, GD4, MS4 and the maximum number iterations of the CT4 (CV4 < 0.1, GD4 < 0.001 and MS4 > 0.9) in Fig. 11(e), (f), which in weighted averaging three types of dynamic communication environments. We find that the CV4, GD4 and CT4 of the dynamic strategies are smaller than that of the static strategies, and the MS4 value of the dynamic strategy is larger than of the static strategy. Therefore, by the above analysis, the dynamic

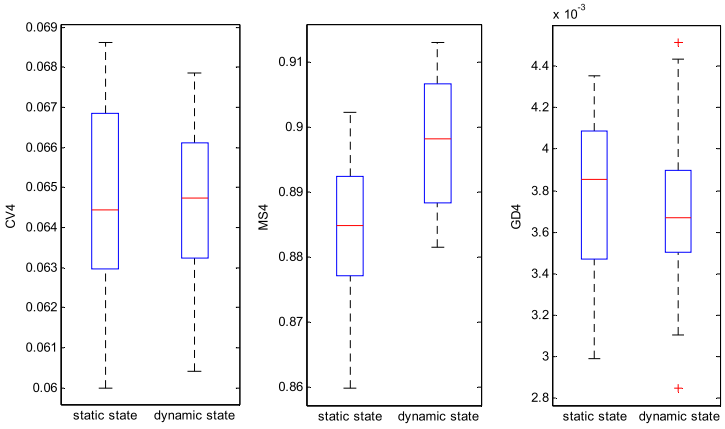

(d) the average performance of CV, MS and GD

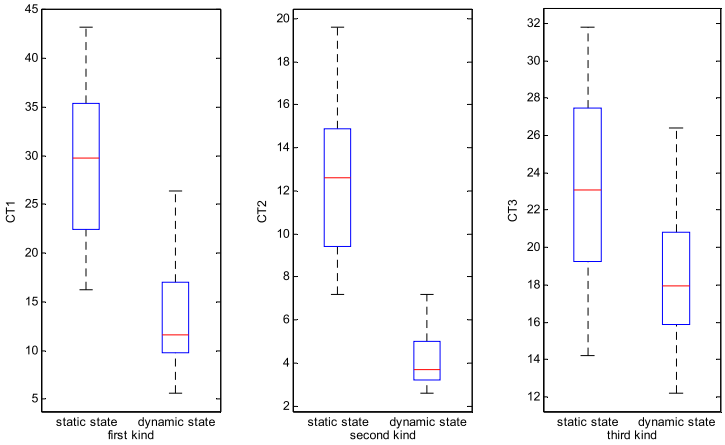

(e) the maximum number of iterationsCT1-3 (CV<0.1, GD<0.001 and MS>0.9)

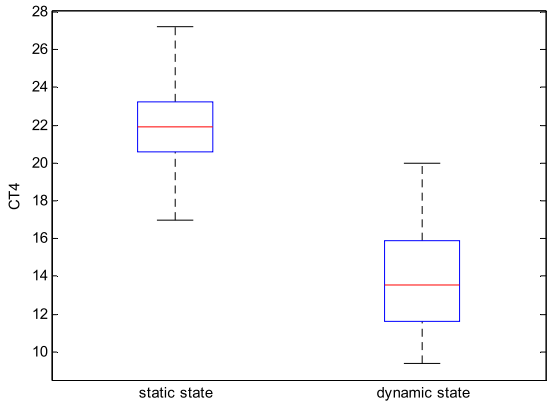

(f) the average maximum number of iterations CT4 (CV<0.1, GD<0.001 and MS>0.9)

Fig. 11. (*continued*).

strategy can use historical information to accelerate the convergence speed of the ICMOPSO algorithm and help PUs and SUs more quickly adapt to the dynamic communication environment. In general, the dynamic response strategy is better than the static strategy in ICMOPSO algorithm.

From Fig. 11 and Table 7, we conclude that the power control scheme based on the dynamic response strategy has the better ability of adapting to the dynamic environment and smaller calculation compared with the static response strategy.

5. Conclusion

In this paper, a power control scheme based on IMOPSO algorithm is proposed in underlay cognitive radio network. Our optimization object is to maximize throughput of PUs and SUs under the constraints of maximum interference from SUs of each PU, the minimum SINR of PUs and SUs as well as power restriction of communication devices for all users. In order to obtain a better diversity of throughput allocation scheme, the power control scheme based on ICMOPSO algorithm is proposed in order to ensure the QoS of users. Moreover, for the purpose of adapting to dynamic environment, three types of dynamic response strategies

Table 7
Performances of the dynamic and static response strategies in three types of environments.

Performance evaluation	Response strategy	Minimum value	Average value	Maximum value	Variance
CV1	Static response strategy	0.0593	0.0661	0.0731	0.0000
	Dynamic response strategy	0.0540	0.0672	0.0773	0.0000
CV2	Static response strategy	0.0544	0.0614	0.0705	0.0000
	Dynamic response strategy	0.0558	0.0617	0.0663	0.0000
CV3	Static response strategy	0.0557	0.0653	0.0718	0.0000
	Dynamic response strategy	0.0608	0.0649	0.0712	0.0000
CV4	Static response strategy	0.0600	0.0645	0.0686	0.0000
	Dynamic response strategy	0.0604	0.0647	0.0679	0.0000
GD1	Static response strategy	0.0031	0.0055	0.0075	0.0000
	Dynamic response strategy	0.0038	0.0056	0.0092	0.0000
GD2	Static response strategy	0.0010	0.0019	0.0031	0.0000
	Dynamic response strategy	0.0009	0.0019	0.0026	0.0000
GD3	Static response strategy	0.0028	0.0038	0.0048	0.0000
	Dynamic response strategy	0.0028	0.0037	0.0044	0.0000
GD4	Static response strategy	0.0030	0.0038	0.0044	0.0000
	Dynamic response strategy	0.0028	0.0037	0.0045	0.0000
MS1	Static response strategy	0.8152	0.8540	0.8915	0.0004
	Dynamic response strategy	0.8322	0.8800	0.9135	0.0005
MS2	Static response strategy	0.8699	0.9267	0.9584	0.0004
	Dynamic response strategy	0.9160	0.9447	0.9588	0.0001
MS3	Static response strategy	0.8361	0.8784	0.9087	0.0004
	Dynamic response strategy	0.8534	0.8828	0.9020	0.0002
MS4	Static response strategy	0.8598	0.8844	0.9022	0.0001
	Dynamic response strategy	0.8815	0.8976	0.9130	0.0001
CT1	Static response strategy	16.2000	29.2600	43.2000	70.4552
	Dynamic response strategy	5.6000	13.7900	26.4000	35.3578
CT2	Static response strategy	7.2000	12.6300	19.6000	13.9927
	Dynamic response strategy	2.6000	4.0900	7.2000	1.4883
CT3	Static response strategy	14.2000	23.0600	31.8000	25.4636
	Dynamic response strategy	12.2000	18.6450	26.4000	13.6289
CT4	Static response strategy	16.9500	22.0025	27.2000	7.1612
	Dynamic response strategy	9.4000	13.7925	20.0000	7.9343

represents the superior performance.

are proposed based on ICMOPSO algorithm. Finally, the simulation results show that the power control scheme of ICMOPSO algorithm is better than IMOPSO algorithm and obtain the maximum throughput of PUs and SUs as well as satisfy the constraint of the QoS of PUs and SUs. The archive management based on improved crowding distance of ICMOPSO algorithm supplies more throughput allocation schemes for the decision maker, which is better than that of other algorithms. From the performance of CV, GD and MS, ICMOPSO algorithm is better than IMOPSO algorithm, IMOCPSO algorithm and IMOQPSO algorithm. In addition, the dynamic response strategy based on ICMOPSO algorithm can adapt to the time-varying dynamic environment and need less computation cost.

In the future, we expect to improve the global search ability and reduce the computational cost in multi-objective evolutionary algorithms, which can provide SUs and PUs with more diverse decision-making schemes.

Acknowledgments

This work is supported in part by the National Natural Science Foundation of China under grant no. 61571209 and 61501059, Science and Technology Department of Jilin Provincial, China (Grant No. 20180101336JC) scientific research fund of Jilin Provincial Education Department, China (Grant No. 2016134), outstanding youth fund of Jilin City Science and Technology Bureau, China (Grant No. 20166019), scientific research project of Jilin Institute of Chemical Technology, China (Grant No. 2015128(D)), and major scientific research project of Jilin Institute of Chemical Technology, China (Grant No. 2015010).

Declaration of competing interest

The authors declared that they had no conflicts of interest with respect to their authorship or the publication of this article.

References

[1] Y.C. Liang, K.C. Chen, G.Y. Li, P. Mähönen, Cognitive radio networking and communications: An overview, IEEE Trans. Veh. Technol. 60 (7) (2011) 3386–3407, http://dx.doi.org/10.1109/TVT.2011.2158673.
[2] L.L. Chen, X.H. Zhao, An improved power control AFSA for minimum interference to primary users in cognitive radio networks, Wirel. Pers. Commun. 87 (1) (2016) 0929–6212, http://dx.doi.org/10.1007/s11277-015-3043-5.
[3] L.L. Chen, X.H. Zhao, Power control algorithm for cognitive radio based on chaos particle swarm optimization, J. Inf. Comput. Sci. 11 (12) (2014) 4277–4287, http://dx.doi.org/10.12733/jics201042.
[4] L.L. Chen, X.H. Zhao, Power control algorithm based on dynamic particle swarm optimization in cognitive radio networks, J. Comput. Inf. Syst. 11 (8) (2015) 2863–2872, http://dx.doi.org/10.12733/jcis13939.
[5] X. Zhang, X. Zhang, J population-adaptive differential evolution-based power allocation algorithm for cognitive radio networks, EURASIP J. Wireless Commun. Networking 2016 (2016) 219, http://dx.doi.org/10.1186/s13638-016-0722-1.

[6] C.a.C. Coello, G.T. Pulido, M.S. Lechuga, Handling multiple objectives with particle swarm optimization, IEEE Trans. Evol. Comput. 8 (3) (2014) 256–279, http://dx.doi.org/10.1109/TEVC.2004.826067.
[7] Y. Wang, Y. Li, Y. Zheng, et al., A linear weighted sum multi-objective optimization algorithm based on PSO for wideband spectrum sensing, Int. J. Online Eng. 11 (9) (2015) 9, http://dx.doi.org/10.3991/ijoe.v11i9.5058.
[8] K.K. Anumandla, B. Akella, S.L. Sabat, et al., Spectrum allocation in cognitive radio networks using multi-objective differential evolution algorithm, in: International Conference on Signal Processing and Integrated Networks, IEEE, 2015, pp. 264–269, http://dx.doi.org/10.1109/SPIN.2015.7095314.
[9] Wen Chen, Tao Li, Tao Yang, Intelligent control of cognitive radio parameter adaption: Using evolutionary multi-objective algorithm based on user preference, Ad Hoc Netw. 26 (2015) 3–16, http://dx.doi.org/10.1016/j.adhoc.2014.09.006.
[10] A. Carlisle, G. Dozier, Adapting particle swarm optimization to dynamic environments, in: International Conference on Artificial Intelligence, 2000, pp. 429–434.
[11] K. Deb, B.R.N. Udaya, S. Karthik, Dynamic multi-objective optimization and decision-making using modified NSGA-II: A case study on hydro-thermal power scheduling, in: International Conference on Evolutionary Multi-Criterion Optimization, EMO 2007: Evolutionary Multi-Criterion Optimization, pp. 803–817. http://dx.doi.org/10.1007/978-3-540-70928-2_60.
[12] A. Zhou, Y. Jin, Q. Zhang, B. Sendhoff, E. Tsang, Prediction-Based Population Re-initialization for Evolutionary Dynamic Multi-objective Optimization, International Conference on Evolutionary Multi-Criterion Optimization, EMO 2007: Evolutionary Multi-Criterion Optimization, pp. 832–846. http://dx.doi.org/10.1007/978-3-540-70928-2_62.
[13] Arrchana Muruganantham, Yang Zhao, Sen. Bong Gee, Xin Qiu, Kay. Chen Tan, Dynamic multiobjective optimization using evolutionary algorithm with Kalman filter, Procedia Comput. Sci. 24 (2013) 66–75, http://dx.doi.org/10.1016/j.procs.2013.10.028.
[14] Yonas G. Woldesenbet, Gary G. Yen, Dynamic evolutionary algorithm with variable relocation, IEEE Trans. Evol. Comput. 13 (3) (2009) 500–513, http://dx.doi.org/10.1109/TEVC.2008.2009031.
[15] Sen Bong Gee, Kay Chen Tan, Cesare Alippi, Solving multiobjective optimization problems in unknown dynamic environments: an inverse modeling approach, IEEE Trans. Cybern. 47 (12) (2017) http://dx.doi.org/10.1109/TCYB.2016.2602561.
[16] Biao Xu, Yong Zhang, Dunwei Gong, Yinan Guo, Miao Rong, Environment sensitivity-based cooperative co-evolutionary algorithms for dynamic multi-objective optimization, IEEE/ACM Trans. Comput. Biol. Bioinform. 15 (6) (2018) 4223–4234, http://dx.doi.org/10.1109/TCYB.2016.2602561.
[17] Ying-Chang Liang, Yonghong Zeng, E.C.Y. Peh, Anh Tuan Hoang, Sensing-throughput tradeoff for cognitive radio networks, IEEE Trans. Wirel. Commun. 7 (4) (2008) 1326–1337, http://dx.doi.org/10.1109/twc.2008.060869.
[18] O.A.H. Al-Tameemi, M. Chatterjee, Capacity of finite secondary cognitive radio networks: Bounds and optimizations, Comput. Commun. 113 (2017) 62–77, http://dx.doi.org/10.1016/j.comcom.2017.09.013.
[19] G. Peng, Y.W. Fang, W.S. Peng, D. Chai, Y. Xu, Multi-objective particle optimization algorithm based on sharing-learning and dynamic crowding distance, Optik 127 (12) (2016) 5013–5020, http://dx.doi.org/10.1016/j.ijleo.2016.02.045.
[20] Dasheng Liu, K.C. Tan, C.K. Goh, W.K. Ho, A multiobjective memetic algorithm based on particle swarm optimization, IEEE Trans. Syst. Man Cybern. B 37 (1) (2007) 42–50, http://dx.doi.org/10.1109/TSMCB.2006.883270.
[21] K. Deb, R. Datta, A bi-objective constrained optimization algorithm using a hybrid evolutionary and penalty function approach, Eng. Optim. 45 (5) (2013) 503–527, http://dx.doi.org/10.1080/0305215X.2012.685074.
[22] A.E. Dawoud, A.A. Rosas, M. Shokair, et al., PSO-adaptive power allocation for multiuser GFDM-based cognitive radio networks, in: 2016 International Conference on Selected Topics in Mobile & Wireless NETWORKING, MoWNeT, IEEE, 2016, http://dx.doi.org/10.1109/MoWNet.2016.7496602.
[23] Q. Lin, J. Li, Z. Du, J. Chen, Z. Ming, A novel multi-objective particle swarm optimization with multiple search strategies, European J. Oper. Res. 247 (3) (2015) 732–744, http://dx.doi.org/10.1016/j.ejor.2015.06.071.
[24] R. Liu, J. Li, J. fan, C. Mu, L. Jiao, A coevolutionary technique based on multi-swarm particle swarm optimization for dynamic multi-objective optimization, European J. Oper. Res. 261 (3) (2017) 1028–1051, http://dx.doi.org/10.1016/j.ejor.2017.03.048.
[25] Z.-H. Zhan, J. Li, J. Cao, J. Zhang, H.S.-H. Chung, Y.-H. Shi, Multiple populations for multiple objectives: a coevolutionary technique for solving multiobjective optimization problems, IEEE Trans. Cybern. 43 (2) (2013) http://dx.doi.org/10.1109/TSMCB.2012.2209115.
[26] Q.Z. Zhang, L.I. Wei-Xiao, L.X. Sha, Drilling parameters optimization based on chaotic multi-objective particle swarm optimization algorithm, in: 2017 International Conference on Electrical Engineering and Automation Control, ICEEAC 2017.
[27] Z.L.Z. Li, K.X.K. Xu, S.L.S. Liu, K.L.K. Li, Quantum multi-objective evolutionary algorithm with particle swarm optimization method, in: 2008 Fourth International Conference on Natural Computation, vol. 3, IEEE, 2008, pp. 672–676, http://dx.doi.org/10.1109/ICNC.2008.785.

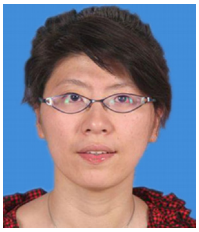

Lingling Chen received her Bachelor and PH.D degrees both in Communication Engineering from Jilin University, China, in 2004 and 2015 respectively. Currently, she is a associate professor of College of Information and Control Engineering, Jilin Institute of Chemical Technology. Simultaneously she is a post-doctor in Computer Science and Technology from Jilin University. Her research interests are in nonlinear optimization, mobile computing and cognitive radio networks. E-mail: cll807900@163.com.

Qi Li received his Bachelor degree in Electronic Information Engineering from Jilin Institute of Chemical Technology, China, in 2018. Currently, he is engaged in intelligent scheduling. His research interests are heuristic algorithms and cognitive radio networks. E-mail: m15044274156@163.com.

Xiaohui Zhao received his Bachelor and Master degrees both in Electrical Engineering from Jilin University of Technology, China,in 1982 and 1986 respectively, and his Ph.D. degree in control theory from University de Technology de Compiegne, in 1993, France. Currently, he is a Professor of College of Communication Engineering, Jilin University. His research interests are signal processing, nonlinear optimization and wireless communication.

Zhiyi Fang received his PhD degree in computer science from Jilin University, Changchun, China, in 1998, where he is currently a professor of computer science. He was a senior visiting scholar of the University of Queensland, Australia, from1995 to 1996, and the University of California, Santa Barbara, from 2000 to 2001. He is a member of China Software Industry Association(CSIA) and a member of Open System Committee of China Computer Federation (CCF). His research interests include distributed/parallel computing system, mobile communication, and wireless networks. E-mail: fangzy@jlu.edu.cn.

Furong Peng received her Bachelor degree in Electronic Information Engineering from Jilin Institute of Chemical Technology, China, in 2018. She is a graduate student at the Tianjin University of Technology and Education. Her research interests are in robust optimization and cognitive radio networks. E-mail: 569206055@qq.com.

Jiaqi Wang will receive her Bachelor degree in Electronic Information Engineering from Jilin Institute of Chemical Technology, China, in 2019. Currently, she is a student of College of Information and Control Engineering, Jilin Institute of Chemical Technology. Her research interests are in tensor analysis and cognitive radio networks. E-mail: 1516730207@qq.com.